Synthesis, Structure, and Bonding of the $[Fe_4(NO)_4(\mu_3\text{-}S)_2(\mu_3\text{-}NCMe_3)_2]^n$ Series (n = 0, −1) Containing a Cubane-Like $Fe_4S_2N_2$ Core: Stereochemical Influence due to One-Electron Reduction of a Completely Bonding Tetrahedral Metal System

Cynthia Ting-Wah Chu, Robert S. Gall, and Lawrence F. Dahl*

Contribution from the Department of Chemistry, University of Wisconsin, Madison, Wisconsin 53706. *Received November 3, 1980. Revised Manuscript Received September 9, 1981*

Abstract: The preparations, spectral properties, structures, and resulting bonding implications of the cubane-like $Fe_4(NO)_4(\mu_3\text{-}S)_2(\mu_3\text{-}NCMe_3)_2$ molecule and its monoanion as the bis(triphenylphosphine) iminium salt are reported. The neutral tetrairon cluster was obtained accidentally in an attempt to prepare the (as yet) unknown iron analogue of the previously characterized cubane-like $Co_4(NO)_4(\mu_3\text{-}NCMe_3)_4$ molecule by the reaction of $Hg[Fe(CO)_3NO]_2$ with $(Me_3CN)_2S$ in refluxing benzene. An X-ray diffraction study of this molecular compound containing an unprecendented cubane-like $Fe_4S_2N_2$ core has allowed an assessment of the stereochemical effect of the electronically equivalent S- and RN-bridged ligands on a completely bonding iron tetrahedron within the same molecule. A subsequent structural determination of its monoanion, generated by the reduction of the neutral parent with Na/Hg amalgam in THF and isolated after an exchange of the PPN^+ cation for the Na^+ ion in solution, has provided an operational test from a comparative geometrical analysis in experimentally differentiating between two possible limiting configurations (suggested by a qualitative MO metal cluster model) upon the addition of an electron to a completely bonding tetrahedral metal system. The neutral tetramer experimentally conforms to C_{2v}—$2mm$ symmetry with one mirror plane crystallographically required; no variations in the resulting two sets of either the Fe–S or Fe–N bond lengths are observed (i.e., both sets have the same means of 2.22 and 1.91 Å, respectively). The geometry of the Fe_2S_2 face (possessing an Fe–Fe single-bond length of 2.642 (1) Å) of the $Fe_2S_2N_2$ core is virtually identical (within 0.01 Å and 0.5°) with that of the six equivalent Fe_2S_2 faces of the Fe_4S_4 core in $Fe_4(NO)_4(\mu_3\text{-}S)_4$; the geometry of the Fe_2N_2 face, for which the Fe–Fe single-bond length of 2.496 (1) Å is expectedly shorter by 0.15 Å, likewise compares favorably with that of the two (Fe–Fe)-bonded Fe_2N_2 fragments in $Fe_3(CO)_9(\mu_3\text{-}NMe)_2$ (which contains an isosceles iron triangle with one nonbonding edge). The intermediate Fe–Fe bond lengths of mean 2.562 Å in the four chemically equivalent Fe_2SN faces correspond to the calculated mean (2.57 Å) of the Fe–Fe bond lengths for the Fe_2S_2 and Fe_2N_2 faces. The monoanion, which retains the idealized C_{2v}—$2mm$ architecture, exhibits relatively large Fe–Fe bond-length increases of 0.059 Å in the Fe_2S_2 face and 0.056 Å in the Fe_2N_2 face in contrast to a smaller average increase of 0.012 Å in each of the four chemically equivalent Fe_2SN faces. A concomitant *lengthening* of the four equivalent Fe–S bonds in the Fe_2S_2 face and two equivalent Fe–S bonds in the Fe_2SN faces by 0.025 and 0.038 Å, respectively, is counterbalanced by a *shortening* of the four equivalent Fe–N bonds in the Fe_2N_2 face and two equivalent Fe–N bonds in the Fe_2SN faces by 0.016 and 0.057 Å, respectively. The determined preferential lengthening of only *two* of the six Fe–Fe bond lengths in the monoanion is compatible with the unpaired electron occupying a MO possessing significant antibonding tetrairon orbital character which is primarily localized within the Fe_2S_2 and Fe_2N_2 faces. In the limiting case where the Fe–Fe bond-length changes are confined to the Fe_2S_2 and Fe_2N_2 faces, the assumed decrease in *total* Fe–Fe bond order from 6.0 in the neutral parent to 5.5 in its monoanion corresponds to each of the two Fe–Fe bonds normal to the C_2 axis decreasing its bond order from unity to $^3/_4$ while the other four chemically equivalent Fe–Fe bonds preserve their individual bond orders of unity. These results suggest that a similar one-electron reduction of the cubic T_d—$\bar{4}3m$ $Fe_4(NO)_4(\mu_3\text{-}S)_4$ molecule should produce (via a first-order Jahn–Teller effect) a tetragonally distorted monoanion of D_{2d}—$\bar{4}2m$ configuration with two relatively longer Fe–Fe bonds normal to the S_4—$\bar{4}$ axis. $Fe_4(NO)_4(\mu_3\text{-}S)_2(\mu_3\text{-}NCMe_3)_2$: monoclinic; $P2_1/m$; a = 11.140 (2) Å, b = 11.013 (2) Å, c = 7.921 (1) Å, β = 91.819 (6)°; V = 971.4 Å^3; ρ(obsd) = 1.85 (5) g cm^{-3} vs. ρ(calcd) = 1.89 g cm^{-3} for Z = 2. Least-squares refinement converged at $R_1(F)$ = 3.3%, $R_2(F)$ = 4.6% for 1194 independent diffractometery data ($I \geq 2\sigma(I)$). $[(Ph_3P)_2N]^+[Fe_4(NO)_4(\mu_3\text{-}S)_2(\mu_3\text{-}NCMe_3)_2]^-$: monoclinic; $P2_1/n$; a = 22.817 (11) Å, b = 10.705 (3) Å, c = 20.596 (5) Å, β = 99.94 (3)°; V = 4955.2 Å^3; ρ(obsd) = 1.44 g cm^{-3} vs. ρ(calcd) = 1.47 g cm^{-3} for Z = 4. Least-squares refinement gave $R_1(F)$ = 9.1%, $R_2(F)$ = 8.2% for 1758 independent diffractometry data ($I \geq 2\sigma(I)$).

The work reported herein originated from our quest to prepare the now-known cubane-like $Fe_4(NO)_4(\mu_3\text{-}S)_4$[1] and/or the (as yet) unknown electronically equivalent $Fe_4(NO)_4(\mu_3\text{-}NCMe_3)_4$ analogue, both of which were presumed from electronic considerations to possess a completely bonding iron tetrahedron. Our interest in the synthesis and structural characterization by X-ray diffraction of the latter tetramer stemmed from a desire to provide an operational test in distinguishing between a possible second-order Jahn–Teller effect vs. unusual intramolecular steric effects of the triply bridging *N-tert*-butyl ligands as a rationalization for the Co_4N_4 core in the $Co_4(NO)_4(\mu_3\text{-}NCMe_3)_4$ tetramer[2] being distorted from tetragonal D_{2d}—$\bar{4}2m$ to orthorhombic D_2—222 symmetry. Instead, the reaction of $(Me_3CN)_2S$ with $Hg[Fe(CO)_3NO]_2$ unexpectedly gave rise to the cubane-like $Fe_4(NO)_4(\mu_3\text{-}S)_2(\mu_3\text{-}NCMe_3)_2$ molecule which, along with the subsequently prepared $Fe_4(NO)_4(\mu_3\text{-}S)_4$ molecule, allows an assessment of geometrical differences between the electronically equivalent S- and Me_3CN-bridged ligands on the completely bonding iron core.

The fact that cyclic voltammetric measurements indicated that both the cubane-like $Fe_4(NO)_4(\mu_3\text{-}S)_4$ and $Fe_4(NO)_4(\mu_3\text{-}S)_2(\mu_3\text{-}NCMe_3)_2$ molecules could be reduced to monoanions was especially encouraging in that we then felt that a comparative analysis of the geometry of either monoanion with that of its neutral parent would establish the validity of our qualitative molecular orbital cluster model[3] which has been utilized to describe the bonding and to discriminate among the different electronic

(1) Gall, R. S.; Chu, C. T.-W.; Dahl, L. F. *J. Am. Chem. Soc.* **1974**, *96*, 4019–4023.
(2) Gall, R. S.; Connelly, N. G.; Dahl, L. F. *J. Am. Chem. Soc.* **1974**, *96*, 4017–4019.
(3) (a) Teo, B. K. Ph.D. Thesis, University of Wisconsin—Madison, 1973. (b) Dahl, L. F. "Abstracts of Papers", 165th National Meeting of the American Chemical Society, Dallas, TX, April 1973; American Chemical Society: Washington, D.C., 1973; INOR 6. (c) Teo, B. K.; Dahl, L. F., to be puslished.

0002-7863/82/1504-0737$01.25/0 © 1982 American Chemical Society

configurations of the cubane-like $Fe_4(NO)_4(\mu_3\text{-}S)_4$,[1] $[Fe_4(\eta^5\text{-}C_5H_5)_4(\mu_3\text{-}S)_4]^n$ (n = 0,[4] 1,[5] 2[6]), and $[Fe_4(SR)_4(\mu_3\text{-}S)_4]^n$ anions (n = −1, −2, −3).[7] This bonding model suggests that a one-electron reduction of the cubic T_d—$\bar{4}3m$ $Fe_4(NO)_4(\mu_3\text{-}S)_4$ molecule to its monoanion would result in the addition of an electron to a triply degenerate antibonding metal cluster orbital which is presumed via a first-order Jahn–Teller distortion to lower the symmetry of the Fe_4S_4 core to a tetragonal D_{2d} geometry with a relative lengthening of either *two* or *four* of the six Fe–Fe distances.[3]

Of particular interest was whether this postulated tetragonal deformation from cubic T_d symmetry is mirror related to the cubane-like $[Co_4(\eta^5\text{-}C_5H_5)_4(\mu_3\text{-}S)_4]^n$ series (n = 0, 1)[8] in which a one-electron oxidation of the nonbonding tetrahedral metal system (of cubic T_d symmetry) in the neutral parent effectively results in the removal of an antibonding metal cluster electron to produce via a first-order Jahn–Teller distortion a flattened tetragonal D_{2d} Co_4S_4 core with four shorter and two longer Co–Co distances.

Substantial efforts to isolate single crystals of the $[Fe_4(NO)_4(\mu_3\text{-}S)_4]^-$ monoanion for X-ray diffraction examination were initially unsuccessful.[9] These attempts included the unexpected isolation and structural redetermination[10] of the classical Roussin black $[Fe_4(NO)_7(\mu_3\text{-}S)_3]^-$ monoanion[11] as an unanticipated decomposition product of the $[Fe_4(NO)_4(\mu_3\text{-}S)_4]^-$ monoanion.

However, our simultaneous efforts to isolate the $[Fe_4(NO)_4(\mu_3\text{-}S)_2(\mu_3\text{-}NCMe_3)_2]^-$ monoanion in crystalline form for an X-ray diffraction study were successful after reactions of the neutral parent with several common reducing agents. Its reaction with Na/Hg amalgam in THF at room temperature was found to give an anionic species, for which solution IR spectra expectedly exhibited lower terminal nitrosyl stretching frequencies relative to the corresponding ones in IR spectra of the neutral parent. The bis(triphenylphosphine) iminium cation was exchanged for the sodium cation in solution in order to stabilize the monoanion in solid-state form, and the insoluble product was purified and then recrystallized by solvent diffusion. A subsequent crystallographic investigation has revealed the heretofore unknown geometrical influence of a one-electron reduction of a completely bonding tetrahedral metal system. A preliminary account of the preparation and structural determination of the neutral $Fe_4(NO)_4(\mu_3\text{-}S)_2(\mu_3\text{-}NCMe_3)_2$ molecule has been presented.[1]

Experimental Section

Preparation and Properties. (a) General Comments. All reactions including reductions, column-chromatographic separations, and crystallizations were carried our under nitrogen or argon in deaerated solvents with Schlenk glassware which was cleaned by standard chromic acid solution and then dried at 120 °C. Reagent grade solvents were dried by standard procedures before use. Na/Hg amalgams were prepared by the King procedure.[12a]

(b) $Fe_4(NO)_4(\mu_3\text{-}S)_2(\mu_3\text{-}NCMe_3)_2$. This tetramer was prepared by the reaction of 10 g of $Hg[Fe(CO)_3NO]_2$[12b] with an excess of $(Me_3CN)_2S$[13] under reflux in benzene for 2 h. Upon cooling, the resultant dark brown solution was filtered to remove any precipitate and then evaporated to dryness. The solid was extracted with hexane. After evaporation of the hexane, the solid was dissolved in cyclohexane and added to a silica gel column. Elution with cyclohexane yielded two bands, the first of which was subsequently identified as $Fe_4(NO)_4(\mu_3\text{-}S)_2(\mu_3\text{-}NCMe_3)_2$.

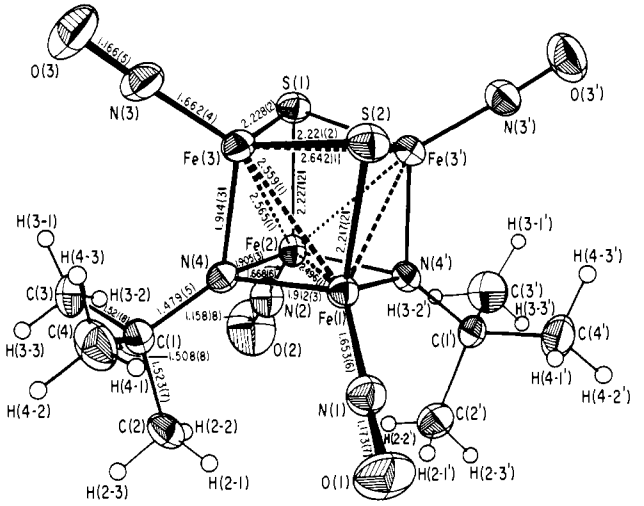

Figure 1. The cubane-like $Fe_4(NO)_4(\mu_3\text{-}S)_2(\mu_3\text{-}NCMe_3)_2$ molecule of idealized C_{2v}—$2mm$ geometry with crystallographic site symmetry C_s—m is drawn with 30% probability thermal ellipsoids for the nonhydrogen atoms.

The expected diamagnetism of $Fe_4(NO)_4(\mu_3\text{-}S)_2(\mu_3\text{-}NCMe_3)_2$ is in accordance with the observation of a sharp singlet in the ^1H NMR spectrum of CCl_4 solution at δ 1.48 (vs. Me_4Si internal standard). A solid-state (KBr) infrared spectrum (Beckman IR-10 spectrometer) revealed three nitrosyl bands at 1792 (w), 1760 (vs), and 1745 (s) cm^{-1}.

(c) $[(Ph_3P)_2N]^+[Fe_4(NO)_4(\mu_3\text{-}S)_2(\mu_3\text{-}NCMe_3)_2]^-$. In a typical experiment, a 150-mL THF solution containing a 0.1-g sample of $Fe_4(NO)_4(\mu_3\text{-}S)_2(\mu_3\text{-}NCMe_3)_2$ was added dropwise to a Na/Hg amalgam (2.3 mL of Hg to 0.3 g of Na) in 100 mL of THF. The reaction mixture was stirred for 5 min and then was filtered 3 times in order to remove the fine gray precipitate. To the filtrate was added a 0.1-g sample of $(Ph_3P)_2NCl$ in a 50-mL acetone solution. After 30 min of stirring under N_2, the solvent was removed under vacuum and the residue extracted with THF. Black platelike crystals of $[(Ph_3P)_2N]^+[Fe_4(NO)_4(\mu_3\text{-}S)_2(\mu_3\text{-}NCMe_3)_2]^-$ were obtained by slow diffusion with THF and heptane.

A solid-state (KBr pellet) infrared spectrum (obtained by using a DIGILAB FTS-20 Fourier transform spectrometer with a 4.0-cm^{-1} resolution) of this compound exhibited four absorption bands at 1762 (w), 1732 (vw), 1682 (vs), and 1664 (s) cm^{-1}. The observed intensity pattern in the nitrosyl stretching region closely corresponds to that obtained previously for the neutral parent except for the absence of the corresponding 1732 (vw) cm^{-1} band which may be attributed to the much lower resolution of the Beckman spectrometer. The decrease by 30–80 cm^{-1} in the corresponding frequencies of the monoanion is in accord with the monoanion expectedly possessing greater $d\pi(Fe)\rightarrow\pi^*(NO)$ backbonding which in turn produces a weakening of the N–O bonds.

(d) Attempted Synthesis of $Fe_4(NO)_4(\mu_3\text{-}NCMe_3)_4$. Our unsuccessful efforts to prepare this compound by the reaction of $(Me_3CN)_2S$ with $Hg[Fe(CO)_3NO]_2$ included the following variety of boundary conditions: (1) a variation of the molar ratio from 1:2 to 1:1 (i.e., a 1:2 molar ratio was used in the preparation of $Fe_4(NO)_4(\mu_3\text{-}S)_2(\mu_3\text{-}NCMe_3)_2$); (2) a change in the refluxing time from 2 h to 20 h; (3) a change of solvent from toluene (bp 110 °C) to benzene (bp 80 °C); and (4) the addition of triphenylphosphine in order to purge the sulfur by formation of triphenylphosphine sulfide. The only major product from all of the above reactions was found to be the previously characterized $Fe_4(NO)_4(\mu_3\text{-}S)_2(\mu_3\text{-}NCMe_3)_2$.

Another reagent, t-$BuNCl_2$, was also added to $Hg[Fe(CO)_3NO]_2$ in benzene at room temperature, but this reaction produced an insoluble green precipitate which was not further characterized. The t-$BuNCl_2$ was prepared[14] by the reaction of *tert*-butylamine with *tert*-butyl hypochlorite.[15]

X-ray Diffraction Analyses and Structural Refinements. (a) $Fe_4(NO)_4(\mu_3\text{-}S)_2(\mu_3\text{-}NCMe_3)_2$. Preliminary Weissenberg photographs

(4) (a) Wei, C. H.; Wilkes, G. R.; Treichel, P. M.; Dahl, L. F. *Inorg. Chem.* **1966**, *5*, 900–905. (b) Schunn, R. A.; Fritchie, C. J., Jr.; Prewitt, C. T. *Ibid.* **1966**, *5*, 892–899.

(5) Trinh-Toan; Fehlhammer, W. P.; Dahl, L. F. *J. Am. Chem. Soc.* **1977**, *99*, 402–407.

(6) Trinh-Toan; Teo, B. K.; Ferguson, J. A.; Meyer, T. J.; Dahl, L. F. *J. Am. Chem. Soc.* **1977**, *99*, 408–416.

(7) (a) Laskowski, E. J.; Reynolds, J. G.; Frankel, R. G.; Foner, S.; Papalfthymiou, G. C.; Holm, R. H. *J. Am. Chem. Soc.* **1979**, *101*, 6562–6570, and references cited therein. (b) Berg, J. M.; Hodgson, K. O.; Holm, R. H. *Ibid.* **1979**, *101*, 4586–4593, and references cited therein.

(8) Simon, G. L.; Dahl, L. F. *J. Am. Chem. Soc.* **1973**, *95*, 2164–2174.

(9) (a) Chu, C. T.-W. Ph.D. Thesis, University of Wisconsin—Madison, 1977. (b) Lo, F. Y.-K. Ph.D. Thesis, University of Wisconsin—Madison, 1979.

(10) Chu, C. T.-W.; Dahl, L. F. *Inorg. Chem.* **1977**, *16*, 3245–3251.

(11) Johansson, G.; Lipscomb, W. N. *Acta Crystallogr.* **1958**, *11*, 594–598, and references cited therein.

(12) King, R. B. "Organometallic Syntheses"; Academic Press: New York, 1965; Vol. I. (a) p 149; (b) pp 165–166.

(13) Clemens, D. H.; Bell, A. J.; O'Brien, J. L. *Tetrahedron Lett.* **1965**, 1487–1489.

(14) Zimmer, H.; Audrieth, L. F. *J. Am. Chem. Soc.* **1954**, *76*, 3856–3857.

(15) Teeter, H. M.; Bachmann, R. C.; Bell, E. W.; Cowan, J. C. *Ind. Eng. Chem.* **1949**, *41*, 849–852.

showed Laue symmetry C_{2h}—$2/m$. Systematic absences of $k = 2n + 1$ for $\{0k0\}$ indicated the possible space groups $P2_1$ (C_2^2, No. 4) and $P2_1/m$ (C_{2h}^2, No. 11). Our choice of the centrosymmetric space group $P2_1/m$ was substantiated by the successful refinement. A crystal of dimensions 0.50 × 0.22 × 0.22 mm along the [001], [100], and [110] directions, respectively, was wedged into a 0.20-mm capillary which was cemented with epoxy glue to a fiber such that the c axis was approximately parallel to the goniometer spindle axis. The crystal was then mounted and aligned on a Datex-controlled General Electric diffractometer equipped with a full-circle (E&A) goniometer and with a scintillation counter and pulse height analyzer adjusted to admit 90% of the Mo Kα (λ = 0.71069 Å) peak. Twenty carefully centered reflections were used in a least-squares procedure[16a] to calculate 2θ, ϕ, and χ values for the full set of data. The lattice parameters obtained were as follows: a = 11.140 (2) Å, b = 11.013 (2) Å, c = 7.921 (1) Å, and β = 91.819° (6). The volume of the unit cell is 971.4 Å^3. The calculated density of 1.89 g/cm^3, based on two tetrameters per unit cell, agrees with the experimental density of 1.85 (5) g/cm^3.

Intensity data were collected by the θ-2θ scan technique for the independent reciprocal lattice octants hkl and $\bar{h}kl$. Symmetric scans of 1.40° (3.0° < 2θ < 10.0°) and 1.20° (10.0° < 2θ < 45.0°) were employed with 2°/min scans and 12-s background measurements on each side of each peak. Four standard reflections, which were sampled after every 100 reflections, showed no significant changes (>2.0%) in their intensities during the data collection. The intensity of each reflection was measured at least twice; details of the data collection and reduction are given elsewhere.[17] Since the transmission coefficients (based on a calculated linear absorption coefficient of 32.3 cm^{-1} for Mo Kα radiation) varied from 0.50 to 0.56, the data were corrected[16b] for absorption effects. A merging[16c] of the data gave 1194 independent reflections (with $I \geq 2\sigma(I)$) which were used in the structural determination and refinement.

The structure of $Fe_4(NO)_4(\mu_3\text{-}S)_2(\mu_3\text{-}NCMe_3)_2$ was determined by the heavy-atom method. A solution of the Harker vectors on a three-dimensional Patterson map[16d] located (under $P2_1/m$ symmetry) the position of one iron atom (not on a special position) which gave discrepancy factors of $R_1(F)$ = 67.1% and $R_2(F)$ = 76.2%.[18] A Fourier synthesis[16d] phased on this atom yielded the positions of two other iron atoms and two sulfur atoms on the mirror plane at $y = {}^1/_4$. Further Fourier maps[16d] resolved the initial coordinates of all independent nonhydrogen atoms. Least-squares refinement[16e] with isotropic temperature factors for these atoms converged at $R_1(F)$ = 7.7%, $R_2(F)$ = 12.1%; full-matrix anisotropic least squares further reduced the residuals to $R_1(F)$ = 4.1%, $R_2(F)$ = 6.2%. At this point, a Fourier difference map gave reasonable positions for eight of the nine independent hydrogen atoms; the position of the ninth hydrogen atom was idealized with the program MIRAGE.[16f] Least-squares refinement with positional and anisotropic thermal parameters varied for the nonhydrogen atoms and with positional and isotropic temperature factors varied for the hydrogen atoms gave final residuals of $R_1(F)$ = 3.3% and $R_2(F)$ = 4.6%. In these refinements anomalous dispersion corrections for iron ($\Delta F'$ = 0.4, $\Delta F''$ = 1.0)[19] and sulfur ($\Delta F'$ = 0.1, $\Delta F''$ = 0.2) were applied to the neutral scattering factors.[20] A final Fourier difference map revealed no residual peaks greater than 0.6 e/Å^3.

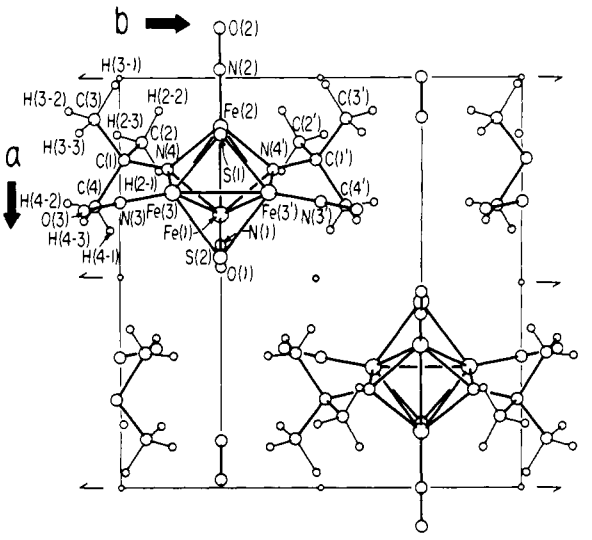

Figure 2. A projection of the monoclinic unit cell of symmetry $P2_1/m$ showing the two $Fe_4(NO)_4(\mu_3\text{-}S)_2(\mu_3\text{-}NCMe_3)_2$ molecules each lying on a mirror plane.

The positional and thermal parameters from the output of the last least-squares cycle are given in Table I. Interatomic distances and bond angles calculated[16g] from the variance–covariance matrix are presented in Table II.[21] Selected least-squares planes and interplanar angles were calculated.[16h] All illustrations were drawn with the aid of ORTEP.[16i]

(b) $[(Ph_3P)_2N]^+[Fe_4(NO)_4(\mu_3\text{-}S)_2(\mu_3\text{-}NCMe_3)_2]^-$. A platelike crystal of dimensions 0.28 × 0.02 × 0.40 mm along the [1$\bar{1}$1], [1$\bar{1}$1], and [111] directions, respectively, was glued with epoxy cement to the end of a glass fiber which was sealed inside an argon-filled Lindemann glass capillary. Preliminary oscillation and Weissenberg photographs showed the crystal to possess monoclinic C_{2h}—$2/m$ Laue symmetry. Systematic absences of $\{h0l\}$ for $h + l$ odd and of $\{0k0\}$ for k odd uniquely defined the probable space group as $P2_1/n$ [nonstandard setting of $P2_1/c$-C_{2h}^5], and this choice was substantiated from the successful structural determination and refinement.

The crystal was aligned on a Syntex P$\bar{1}$ diffractometer, and intensity data were sampled once with Mo Kα radiation via the θ-2θ scan mode for the independent monoclinic octants hkl and $hk\bar{l}$ over the range 3.0° ≤ 2θ ≤ 40.0°. Details of the data collection and reduction are given elsewhere.[22] Transmission coefficients for the crystal, which varied from 0.90 to 0.98, necessitated an absorption correction which was carried out[16b] on the basis of a linear absorption coefficient of 13.6 cm^{-1} for Mo Kα radiation. The corrected data were merged[16e] to yield 1758 independent reflections (with $I \geq 2\sigma(I)$) which were used in the solution and refinement of the structure.

The measured lattice constants for the monoclinic unit cell at ca. 22° are a = 22.817 (11) Å, b = 10.705 (3) Å, c = 20.596 (5) Å, and β = 99.94 (3)°. The unit cell volume is 4955 Å^3. The total number of electrons per unit cell, $F(000)$, is 2276. The observed density of 1.44 g/cm^3, measured by the flotation technique, is in agreement with a calculated density of 1.47 g/cm^3 for Z = 4. All atoms are located in the 4-fold general set of equivalent positions, which for $P2_1/n$ are $\pm(x, y, z; {}^1/_2 + x, {}^1/_2 - y, {}^1/_2 + z)$.

After unsuccessful attempts to determine the positions of the heavy atoms by interpretation of a calculated Patterson map, the four independent iron atoms comprising one tetramer were located from direct methods by the use of MULTAN.[16j] Four subsequent Fourier maps revealed positions for all other nonhydrogen atoms. The hydrogen atoms on the *N-tert*-butyl groups and phenyl rings were then fit[16f] to idealized groups with C-H distances of 1.0 Å. During all further refinements the coordinates of the hydrogen atoms were not varied, but new idealized positions were recalculated from the changed carbon coordinates after

(16) (a) Foust, A. S. "ANGSET"; Ph.D. Thesis, University of Wisconsin—Madison, 1970, Appendix. (b) Blount, J. F. "DEAR, A FORTRAN Absorption-Correction Program"; 1965, based on the method give by: Busing, W. R.; Levy, H. A. *Acta Crystallogr.* **1957**, *10*, 180–182. (c) Calabrese, J. C. "SORTMERGE"; Ph.D. Thesis, University of Wisconsin—Madison, 1971, Appendix. (d) Calabrese, J. C. "MAP, a FORTRAN Summation and Molecular Assemblage Program"; University of Wisconsin—Madison, 1972. (e) "OR FLSR, A Local Rigid-Body Least-Squares Program"; adapted from the Busing-Martin-Levy ORFLS, Report ORNL-TM-305; Oak Ridge National Laboratory, Oak Ridge, TN, 1962. (f) Calabrese, J. C. "MIRAGE"; Ph.D. Thesis, University of Wisconsin—Madison, 1971, Appendix III. (g) Busing, W. R.; Martin, K. O.; Levy, H. A. "OR FFE, A FORTRAN Crystallographic Function and Error Program"; Report ORNL-TM-306, Oak Ridge National Laboratory, Oak Ridge, TN, 1964. (h) "PLANES", a revised version of "PLANE 1" written by: Smith, D. L. Ph.D. Thesis, University of Wisconsin—Madison, 1962, Appendix IV. (i) Johnson, C. K. "OR TEP-II, A FORTRAN Thermal-Ellipsoid Plot Program for Crystal Structure Illustrations"; Report ORNL-5138, Oak Ridge National Laboratory, Oak Ridge, TN, 1976. (j) Main, P.; Lessinger, L.; Woolfson, M. M.; Germain, G.; Declercq, J.-P. "MULTAN-76", an undated version of MULTAN: Germain, G.; Main, P.; Woolfson, M. M. *Acta Crystallogr.* **1971**, *A27*, 368–376. (k) Calabrese, J. C. "A Crystallographic Variable Matrix Least-Squares Refinement Program"; University of Wisconsin—Madison, 1972.

(17) Uchtman, V. A.; Dahl, L. F. *J. Am. Chem. Soc.* **1969**, *91*, 3763–3769.

(18) The unweighted and weighted discrepancy factors used are $R_1(F) = [\sum||F_o| - |F_c||/\sum|F_o|] \times 100$ and $R_2(F) = [\sum w_i||F_o| - |F_c||^2/\sum w_i|F_o|^2]^{1/2} \times 100$. All least-squares refinements were based on the minimization of $\sum w_i||F_o| - |F_c||^2$ with individual weights of $w_i = 1/\sigma^2(F_o)$ assigned on the basis of the esd's of the observed structure factors.

(19) "International Tables for X-Ray Crystallography"; Kynoch Press: Birmingham, England, 1974; Vol. IV, p 149.

(20) (a) Cromer, D. T.; Mann, J. B. *Acta Crystallogr., Sect. A* **1968**, *A24*, 321–324. (b) Stewart, R. F.; Davidson, E. R.; Simpson, W. T. *J. Chem. Phys.* **1965**, *42*, 3175–3187.

(21) A listing of the observed and calculated structure factors is available (without charge) upon request from the Inorganic Secretary, Department of Chemistry, University of Wisconsin—Madison, Madison, WI 53706.

(22) Byers, L. R.; Dahl, L. F. *Inorg. Chem.* **1980**, *19*, 277–284.

Table I. Positional and Thermal Parameters for $Fe_4(NO)_4(\mu_3\text{-}S)_2(\mu_3\text{-}NCMe_3)_2$[a]

A. Positional Parameters

atom	x	y	z
Fe(1)	0.34720 (7)	1/4	0.78325 (10)
Fe(2)	0.13683 (7)	1/4	0.88265 (11)
Fe(3)	0.29855 (6)	0.13004 (6)	0.04923 (8)
S(1)	0.16178 (16)	1/4	0.16272 (20)
S(2)	0.45700 (15)	1/4	0.02168 (22)
O(1)	0.4685 (6)	1/4	0.4752 (8)
O(2)	0.9003 (5)	1/4	0.7426 (11)
O(3)	0.6536 (4)	0.0890 (4)	0.7752 (6)
N(1)	0.4171 (5)	1/4	0.6023 (7)
N(2)	−0.0030 (5)	1/4	0.8008 (8)
N(3)	0.3256 (4)	0.0001 (4)	0.1499 (5)
N(4)	0.2384 (3)	0.1192 (3)	0.8208 (4)
C(1)	0.2120 (4)	0.0111 (4)	0.7154 (6)
C(2)	0.1664 (6)	0.0534 (5)	0.5419 (7)
C(3)	0.8842 (6)	0.0632 (6)	0.1998 (9)
C(4)	0.6751 (7)	0.0628 (6)	0.3019 (10)
H(2-1)	0.2342 (54)	0.0967 (52)	0.4854 (72)
H(2-2)	0.0900 (65)	0.0960 (57)	0.5347 (82)
H(2-3)	0.8537 (53)	0.0082 (53)	0.5307 (79)
H(3-1)	0.8498 (54)	0.1016 (56)	0.0980 (84)
H(3-2)	0.9660 (64)	0.0117 (57)	0.2012 (81)
H(3-3)	0.9044 (54)	0.1278 (58)	0.2643 (79)
H(4-1)	0.6166 (69)	0.0244 (67)	0.3415 (88)
H(4-2)	0.6837 (43)	0.1316 (48)	0.3753 (66)
H(4-3)	0.6363 (60)	0.0889 (58)	0.1892 (89)

B. Thermal Parameters[b]

atom	$\beta_{11} \times 10^4$	$\beta_{22} \times 10^4$	$\beta_{33} \times 10^4$	$\beta_{12} \times 10^4$	$\beta_{13} \times 10^4$	$\beta_{23} \times 10^4$
Fe(1)	50.6 (8)	54.4 (8)	109.4 (16)	0[c]	−3.2 (7)	0
Fe(2)	51.4 (8)	51.1 (8)	119.5 (16)	0	−0.1 (8)	0
Fe(3)	71.0 (7)	64.4 (7)	108.1 (13)	6.3 (4)	8.2 (6)	10.9 (6)
S(1)	88.8 (17)	75.4 (16)	110.3 (28)	0	18.5 (16)	0
S(2)	54.9 (14)	94.2 (18)	152.7 (31)	0	−28.9 (16)	0
O(1)	145 (7)	185 (8)	209 (12)	0	89 (7)	0
O(2)	58 (5)	206 (10)	502 (2)	0	−77 (8)	0
O(3)	187 (6)	117 (5)	271 (9)	55 (4)	36 (6)	86 (6)
N(1)	81 (5)	81 (6)	148 (10)	0	18 (6)	0
N(2)	64 (6)	85 (6)	243 (13)	0	4 (7)	0
N(3)	105 (4)	89 (5)	150 (8)	20 (3)	2 (4)	28 (5)
N(4)	57 (3)	55 (3)	107 (6)	4 (2)	6 (3)	4 (3)
C(1)	86 (4)	50 (4)	138 (8)	2 (3)	7 (5)	11 (5)
C(2)	103 (6)	81 (5)	149 (9)	−11 (6)	−24 (6)	−25 (6)
C(3)	137 (7)	74 (5)	230 (13)	−43 (5)	4 (8)	1 (7)
C(4)	123 (7)	83 (6)	245 (13)	33 (6)	−12 (8)	41 (8)

[a] In this and the following tables the standard deviations of the last significant figures are given in parentheses. [b] The anisotropic thermal parameters are of the form: $\exp[-(\beta_{11}h^2 + \beta_{22}k^2 + \beta_{33}l^2 + 2\beta_{12}hk + 2\beta_{13}hl + 2\beta_{23}kl)]$. The refined isotropic temperature factors ($Å^2$) of the hydrogen atoms are as follows: H(2-1) 5.3 (13), H(2-2) 7.2 (16), H(2-3) 5.5 (13), H(3-1) 6.3 (15), H(3-2) 7.6 (15), H(3-3) 6.2 (16), H(4-1) 8.0 (23), H(4-2) 3.9 (11), H(4-3) 6.3 (15). [c] For those atoms located on the crystallographic mirror plane at $y = 1/4$, anisotropic thermal coefficients β_{12} and β_{23} are required by symmetry to be zero.

every other least-squares cycle. Block-diagonal least-squares refinement[16k] with anisotropic thermal parameters for all nonhydrogen atoms of the monoanion except the *tert*-butyl carbon atoms and with isotropic temperature factors for all nonhydrogen atoms of the bis(triphenylphosphine) iminium cation converged at $R_1(F) = 9.1\%$, $R_2(F) = 8.2\%$. A final full-matrix least-squares cycle,[16e] for which only the positional parameters for all nonhydrogen atoms were varied due to size limitations of the computer used, gave $R_1(F) = 9.1\%$, $R_2(F) = 8.2\%$. A difference Fourier map, which showed the largest positive peak to be less than 0.4 e/$Å^3$, revealed no unusual features. Anomalous dispersion corrections[19] were again made to the scattering factors[20] for iron and sulfur.

The positional and thermal parameters from the output of the final full-matrix least-squares cycle are presented in Table III, while interatomic distances and bond angles[16g] are presented in Table IV.[21] Selected least-squares planes and interplanar angles were obtained,[16h] and ORTEP[16i] was again utilized for all drawings.

Results and Discussion

General Description of the Crystal Structures. (a) $Fe_4(NO)_4(\mu_3\text{-}S)_2(\mu_3\text{-}NCMe_3)_2$. Its solid-state structure is expectedly composed of discrete molecules whose configuration (Figure 1) ideally conforms to C_{2v}—2*mm* symmetry with one vertical mirror plane crystallographically required. The disposition under C_s—*m* site symmetry of the two molecules in the monoclinic unit cell is shown in Figure 2. The closest intermolecular contact of 2.86 (5) Å is between a nitrosyl oxygen atom and a hydrogen atom of the *tert*-butyl substituent on a nitrogen atom. Since this distance is longer than the normal van der Waals values of 2.6 Å, it consequently cannot be constructed as a hydrogen bond. Since all other intermolecular distances less than 3.2 Å are either NO···HC or S···HC contacts, no unusual intermolecular interactions are presumed to exist in the solid state.

(b) $[(Ph_3P)_2N]^+[Fe_4(NO)_4(\mu_3\text{-}S)_2(\mu_3\text{-}NC(CH_3)_3)_2]^-$. Its solid-state structure consists of discrete cations and anions whose arrangement in the unit cell is shown in Figure 3. There is no evidence of any unusual interionic interactions in that the shortest interionic nonhydrogen contacts exceed 3.0 Å with no NO···HC distances being less than 2.6 Å.

The solid-state stereochemistry (Figure 4) of the independent bent bis(triphenylphosphine) iminium monocation (abbreviated PPN^+) is of interest in the case of this particular salt in that its conformation does not at all approximate to the cisoid pentadienyl-type arrangement[23] (of C_2 symmetry) found for most of

(23) Handy, L. B.; Ruff, J. K.; Dahl, L. F. *J. Am. Chem. Soc.* **1970**, *92*, 7327–7337.

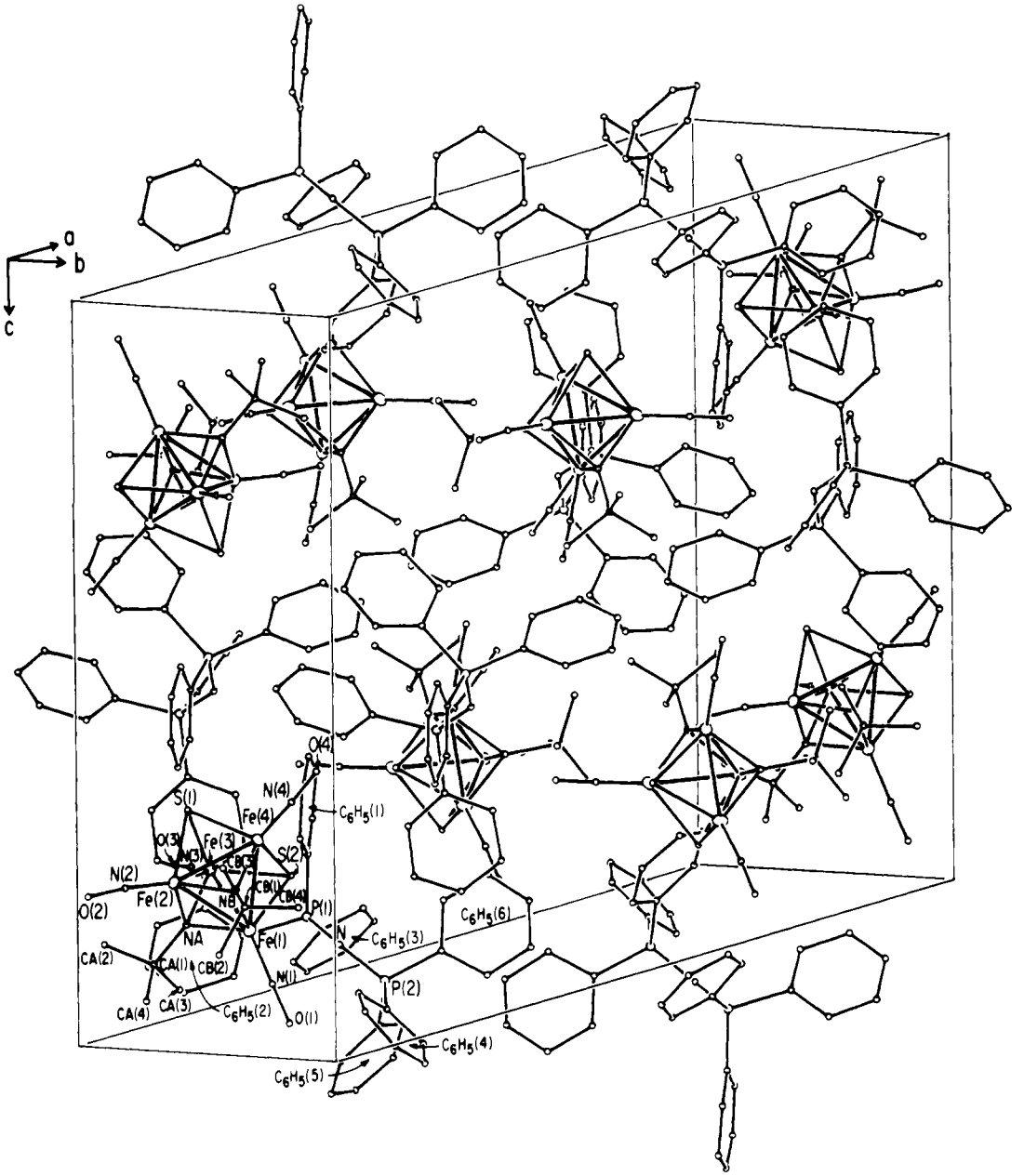

Figure 3. Perspective view of the monoclinic unit cell of $[(Ph_3P)_2N]^+[Fe_4(NO)_4(\mu_3\text{-}S)_2(\mu_3\text{-}NCMe_3)_2]^-$ showing the four cations and four monoanions related by $P2_1/n$ symmetry.

the bent PPN^+ cations in other compounds.[24] This monocation possesses the usually bent P–N–P core in contrast to the linear one observed by Wilson and Bau[25] in the $[V(CO)_6]^-$ salt. The determined P–N–P bond angle of 140 (1)° and N–P distances of 1.57 (2) and 1.58 (2) Å are also analogous to those in other bent PPN^+ cations, with a nearly tetrahedral configuration expectedly being found about each phosphorus atom. The six independent phenyl rings are each coplanar within experimental error (viz., with carbon displacements of ≤0.05 Å from the mean plane). However, Figure 4 indicates (in accordance with a least-squares plane calculation)[26] that the orientation of the six phosphorus-attached phenyl carbon atoms may be described in a gross fashion[26] as a staggered mirror-plane conformation (with the mirror plane defined by the P–N–P core) in which the two phenyl carbon atoms assumed to lie on the mirror plane are oppositely directed to give a staggered conformation along the P···P line. This unprecedented (to our knowledge) solid-state conformation for the PPN^+ cation differs markedly both from the idealized cisoid pentadienyl-type C_2—2 conformation (in which

(24) (a) Handy, L. B.; Ruff, J. K.; Dahl, L. F. *J. Am. Chem. Soc.* **1970**, *92*, 7312–7326. (b) Ruff, J. K.; White, R. P., Jr.; Dahl, L. F. *J. Am. Chem. Soc.* **1971**, *93*, 2159–2176. (c) Smith, M. B.; Bau, R. *J. Am. Chem. Soc.* **1973**, *95*, 2388–2389. (d) Chin, H. B.; Smith, M. B.; Wilson, R. D.; Bau, R. *J. Am. Chem. Soc.* **1974**, *96*, 5285–5287. (e) Goldfield, S. A.; Raymond, K. N. *Inorg. Chem.* **1974**, *13*, 770–775. (f) Chin, H. B.; Bau, R. *Inorg. Chem.* **1978**, *17*, 2314–2317. (g) Petersen, J. L.; Johnson, P. L.; O'Connor, J. P.; Dahl, L. F.; Williams, J. M. *Inorg. Chem.* **1978**, *17*, 3460–3469. (h) Ginsburg, R. E.; Berg, J. M.; Rothrock, R. K.; Collman, J. P.; Hodgson, K. O.; Dahl, L. F. *J. Am. Chem. Soc.* **1979**, *101*, 7218–7231.

(25) Wilson, R. D.; Bau, R. *J. Am. Chem. Soc.* **1974**, *96*, 7601–7602.

(26) Though the orientations of the three phosphorus-attached C(*n*1) atoms of the $C_6H_5(n)$ rings (n = 1, 2, 3) coordinated to P(1) closely adhere to this description, the orientations of the other three phosphorus-linked C(*n*1) atoms of the $C_6H_5(n)$ rings (n = 4, 5, 6) do not. The extent of this variation from the idealized conformational model is indicated by C(31) being displaced by only 0.04 Å from the PNP plane, with C(11) and C(21) being mirror related within a distance difference from the PNP plane of 0.12 Å. On the other hand, C(41) is perpendicularly displaced by 0.56 Å from the PNP plane, and consequently C(51) and C(61) differ by 0.50 Å from being mirror related; these latter deviations correspond to a localized rigid-body rotation of the three phenyl carbon atoms (viz., C(41), C(51), C(61)) from the assumed mirror-plane conformation by ca. 20° about the N–P(2) bond.

Table II. Interatomic Distances and Bond Angles for $Fe_4(NO)_4(\mu_3\text{-}S)_2(\mu_3\text{-}NCMe_3)_2$

A. Intramolecular Distances (Å) with Those for the $Fe_4S_2N_2$ Core Averaged under Assumed C_{2v} Symmetry

Fe(1)-Fe(2)	2.496 (1)	Fe(1)-N(1)	1.653 (6)
Fe(3)-Fe(3')	2.642 (1)	Fe(2)-N(2)	1.668 (6)
		Fe(3)-N(3)	1.662 (4)
Fe(1)-Fe(3)	2.559 (1)		
Fe(2)-Fe(3)	2.565 (1)	N(1)-O(1)	1.173 (7)
	2.562 (av)	N(2)-O(2)	1.158 (8)
		N(3)-O(3)	1.166 (5)
Fe(1)-S(2)	2.217 (2)	N(4)-C(1)	1.479 (5)
Fe(2)-S(1)	2.227 (2)		
	2.222 (av)	C(1)-C(2)	1.523 (7)
		C(1)-C(3)	1.521 (8)
Fe(3)-S(1)	2.228 (2)	C(1)-C(4)	1.508 (8)
Fe(3)-S(2)	2.221 (2)		
	2.224 (av)	C(2)-H(2-1)	1.01 (6)
		C(2)-H(2-2)	0.97 (7)
Fe(3)-N(4)	1.914 (3)	C(2)-H(2-3)	0.91 (6)
		C(3)-H(3-1)	0.98 (7)
Fe(1)-N(4)	1.912 (3)	C(3)-H(3-2)	1.07 (7)
Fe(2)-N(4)	1.905 (3)	C(3)-H(3-3)	0.90 (7)
	1.908 (av)	C(4)-H(4-1)	0.85 (7)
		C(4)-H(4-2)	0.96 (5)
S(1)···S(2)	3.507 (3)	C(4)-H(4-3)	1.02 (7)
N(4)···N(4')	2.880 (7)		
		N(1)···H(2-1)	2.78 (6)
S(1)···N(4)	3.207 (4)	N(1)···H(4-1)	3.08 (7)
S(2)···N(4)	3.208 (4)	N(2)···H(2-2)	2.92 (6)
	3.208 (av)	N(2)···H(3-2)	2.91 (6)
		N(3)···H(3-1)	2.95 (6)
		N(3)···H(4-3)	2.90 (6)

B. Bond Angles (deg) with Those for the $Fe_4S_2N_2$ Core Averaged under Assumed C_{2v} Symmetry

Fe(3)-S(1)-Fe(3')	72.75 (7)	Fe(1)-N(1)-O(1)	178.9 (6)
Fe(3)-S(2)-Fe(3')	73.00 (6)	Fe(2)-N(2)-O(2)	179.4 (7)
	72.88 (av)	Fe(3)-N(3)-O(3)	177.8 (4)
Fe(1)-S(2)-Fe(3)	70.43 (6)	Fe(1)-N(4)-C(1)	129.4 (3)
Fe(2)-S(1)-Fe(3)	70.32 (6)	Fe(2)-N(4)-C(1)	130.2 (3)
	70.38 (av)	Fe(3)-N(4)-C(1)	129.9 (3)
Fe(1)-N(4)-Fe(2)	81.6 (1)	N(4)-C(1)-C(2)	108.5 (4)
Fe(1)-N(4)-Fe(3)	83.9 (1)	N(4)-C(1)-C(3)	108.3 (4)
Fe(2)-N(4)-Fe(3)	84.4 (1)	N(4)-C(1)-C(4)	109.5 (4)
	84.2 (av)	C(2)-C(1)-C(3)	110.1 (5)
		C(2)-C(1)-C(4)	109.8 (5)
S(1)-Fe(3)-S(2)	104.05 (6)	C(3)-C(1)-C(4)	110.6 (5)
N(4)-Fe(1)-N(4')	97.8 (2)		
N(4)-Fe(2)-N(4')	98.2 (2)	H(2-1)-C(2)-H(2-2)	144 (5)
	98.0 (av)	H(2-1)-C(2)-H(2-3)	104 (5)
		H(2-2)-C(2)-H(2-3)	97 (5)
		H(3-1)-C(3)-H(3-2)	123 (5)
S(1)-Fe(3)-N(4)	101.3 (1)	H(3-1)-C(3)-H(3-3)	102 (5)
S(2)-Fe(3)-N(4)	101.5 (1)	H(3-2)-C(3)-H(3-3)	102 (5)
	101.4 (av)	H(4-1)-C(4)-H(4-2)	103 (6)
		H(4-1)-C(4)-H(4-3)	98 (6)
S(1)-Fe(2)-N(4)	101.5 (1)	H(4-2)-C(4)-H(4-3)	109 (5)
S(2)-Fe(1)-N(4)	101.7 (1)		
	101.6 (av)		

the phosphorus-linked carbon atoms of the two twofold-related cisoid phenyl rings are nearly coplanar with the P–N–P core) possessed by a large number of other structurally analyzed PPN^+ cations in the crystalline state and from either the noncisoid staggered C_2 conformation or the noncisoid eclipsed C_s conformation (where the mirror plane bisects the P–N–P core) experimentally found for the PPN^+ cation in the $[Fe(CO)_4C_3H_7]^-$ salt[27] and $[Ni_5(CO)_9(\mu_2\text{-}CO)_3]^{2-}$ salt,[28] respectively. It is evident that packing forces can play a dominant role in determining the overall conformation adopted by the PPN^+ monocation in a given crystalline structure; a detailed examination[23] of the cisoid pen-

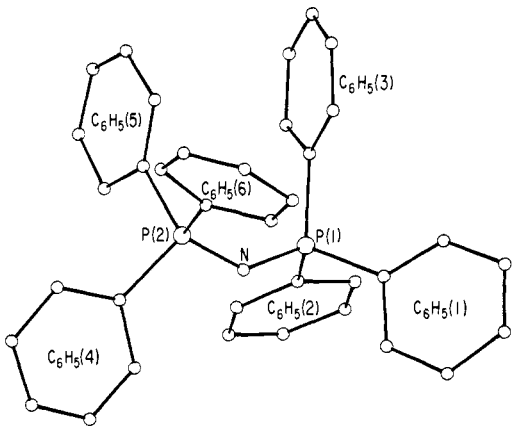

Figure 4. The crystallographically independent bis(triphenylphosphine) iminium cation of $[(Ph_3P)_2N]^+[Fe_4(NO)_4(\mu_3\text{-}S)_2(\mu_3\text{-}NCMe_3)_2]^-$. The six phosphorus-attached phenyl carbon atoms of this unusual solid-state conformation may be conceptually viewed under a gross approximation (see text) as being oriented in a staggered mirror-plane array (with the mirror plane defined by the bent P–N–P core) in which the two carbon atoms, C(31) of $C_6H_5(3)$ and C(41) of $C_6H_5(4)$, assumed to lie on the mirror plane, are oppositely directed to give a staggered conformation along the P···P line.

tadienyl-type C_2—2 conformation observed in different crystal lattices produced the premise that the similar disposition of the phenyl rings found for this particular conformation could be attributed primarily to intra (phenyl ring) steric effects.

The Neutral $Fe_4(NO)_4(\mu_3\text{-}S)_2(\mu_3\text{-}NCMe_3)_2$ Molecule. Stereochemical Effects of *tert*-Butyl Nitrogen vs. Sulfur Bridging Ligands on the Two Types of Localized Iron Environments and Resulting Implications from Mössbauer Spectroscopic Data. This tetrairon cluster (Figure 1) of idealized C_{2v}—2*mm* geometry and crystallographic C_s—*m* site symmetry differs from the closely related $Fe_4(NO)_4(\mu_3\text{-}S)_4$ cluster only by two electronically equivalent, triply bridging *N-tert*-butyl groups being formally substituted in place of two triply bridging sulfur atoms. The configuration of the $Fe_4(NO)_4(\mu_3\text{-}S)_2(\mu_3\text{-}NCMe_3)_2$ molecule may be described as an (Fe–Fe)-bonded Fe_2S_2 moiety joined face-to-face to an (Fe–Fe)-bonded Fe_2N_2 moiety by two Fe–S and two Fe–N bonds and by four electron-pair Fe–Fe bonds to give a cubane-like $Fe_4S_2N_2$ core containing four chemically equivalent (Fe–Fe)-bonded Fe_2SN faces. The geometries of the Fe_2S_2 and Fe_2N_2 faces may be expected to conform reasonably well with those found in other molecules which contain either of these (Fe–Fe)-bonded fragments. In addition, the four Fe_2SN faces may be expected to possess intermediate distances and angles and thereby correspond to an average structure between those of the Fe_2S_2 and Fe_2N_2 faces. Therefore, $Fe_4(NO)_4(\mu_3\text{-}S)_2(\mu_3\text{-}NCMe_3)_2$ presents a unique opportunity (to date) to draw comparisons between S-bridged and RN-bridged structures within the same molecule.

The metal–metal bond lengths divide into three sets which depend upon the kinds of ligands which bridge the metals. For the (Fe–Fe)-bonded Fe_2S_2 face, the Fe–Fe single-bond length of 2.642 (1) Å corresponds closely with the Fe–Fe single-bond lengths of 2.651 (1) Å observed for the six analogous faces in the $Fe_4(NO)_4(\mu_3\text{-}S)_4$ molecule as well as with the mean Fe–Fe distances determined for the two (Fe–Fe)-bonded Fe_2S_2 faces in both orthorhombic $Fe_4(\eta^5\text{-}C_5H_5)_4(\mu_3\text{-}S)_4$ (2.631 (2) Å) and monoclinic $Fe_4(\eta^5\text{-}C_5H_5)_4(\mu_3\text{-}S)_4$ (2.650 Å).

The considerably shorter Fe–Fe single-bond length of 2.496 (1) Å for the Fe_2N_2 face also compares favorably with the mean of the Fe–Fe single-bond lengths determined for the two (Fe–Fe)-bonded Fe_2N_2 fragments in each of the triply bridging, triangular iron complexes $Fe_3(CO)_9(\mu_3\text{-}NMe)_2$ (2.462 (7) Å)[29] and $Fe_3(CO)_9(\mu_3\text{-}NN{=}CPh_2)_2$ (2.44 Å).[30] The remaining two independent Fe–Fe single-bond lengths for the four chemically

(27) Huttner, G.; Gartzke, W. *Chem. Ber.* **1975**, *108*, 1373–1383.
(28) Longoni, G.; Chini, P.; Lower, L. D.; Dahl, L. F. *J. Am. Chem. Soc.* **1975**, *97*, 5034–5036.
(29) Doedens, R. J. *Inorg. Chem.* **1969**, *8*, 570–574.
(30) Baikie, P. E.; Mills, O. S. *Chem. Commun.* **1967**, 1228–1229.

Table III. Atomic Parameters for $[(Ph_3P)_2N]^+[Fe_4(NO)_4(\mu_3\text{-}S)_2(\mu_3\text{-}NCMe_3)_2]^-$ [a]

atom	x	y	z	B, Å²	atom	x	y	z	B, Å²
Fe(1)	0.0155 (2)	0.2936 (4)	0.1740 (2)	b	C(5-6)	−0.3719 (12)	0.6407 (27)	−0.0525 (14)	4.3
Fe(2)	0.1026 (2)	0.3755 (4)	0.2577 (2)	b	C(6-1)	−0.3465 (11)	0.4254 (24)	0.0563 (13)	3.2
Fe(3)	0.0004 (2)	0.4820 (4)	0.2471 (2)	b	C(6-2)	−0.3495 (13)	0.4236 (26)	0.1234 (14)	5.0
Fe(4)	0.0193 (2)	0.2497 (4)	0.2974 (2)	b	C(6-3)	−0.3952 (15)	0.3590 (32)	0.1482 (15)	6.4
S(1)	0.0575 (4)	0.4299 (8)	0.3432 (4)	b	C(6-4)	−0.4334 (14)	0.2925 (31)	0.1043 (18)	6.7
S(2)	−0.0616 (4)	0.3184 (9)	0.2281 (4)	b	C(6-5)	−0.4338 (15)	0.2883 (33)	0.0423 (18)	7.9
NA	0.0514 (9)	0.4527 (19)	0.1867 (10)	b	C(6-6)	−0.3910 (15)	0.3549 (32)	0.0142 (15)	6.6
NB	0.0708 (9)	0.2139 (20)	0.2400 (9)	b	HA(2-1)	0.1413	0.6324	0.1976	c
N(1)	0.0049 (8)	0.2330 (19)	0.1007 (10)	b	HA(2-2)	0.0774	0.7016	0.1966	c
N(2)	0.1728 (11)	0.3961 (22)	0.2667 (11)	b	HA(2-3)	0.1119	0.7162	0.1340	c
N(3)	−0.0277 (11)	0.6218 (27)	0.2413 (12)	b	HA(3-1)	−0.0134	0.5084	0.0687	c
N(4)	0.0084 (11)	0.1429 (29)	0.3478 (13)	b	HA(3-2)	0.0183	0.6406	0.0560	c
O(1)	−0.0022 (8)	0.1841 (20)	0.0469 (9)	b	HA(3-3)	−0.0163	0.6259	0.1186	c
O(2)	0.2255 (9)	0.4123 (25)	0.2672 (11)	b	HA(4-1)	0.0854	0.3925	0.0736	c
O(3)	−0.0500 (11)	0.7241 (24)	0.2355 (12)	b	HA(4-2)	0.1450	0.4414	0.1226	c
O(4)	−0.0006 (9)	0.0681 (22)	0.3886 (10)	b	HA(4-3)	0.1163	0.5248	0.0587	c
CA(1)	0.0684 (14)	0.5405 (29)	0.1356 (15)	5.4	HB(2-1)	0.1702	0.1817	0.1866	c
CA(2)	0.1002 (14)	0.6540 (32)	0.1678 (15)	7.4	HB(2-2)	0.1135	0.1309	0.1336	c
CA(3)	0.0122 (14)	0.5766 (32)	0.0874 (16)	7.7	HB(2-3)	0.1644	0.0332	0.1683	c
CA(4)	0.1090 (13)	0.4716 (28)	0.0978 (14)	6.0	HB(3-1)	0.1827	0.1327	0.3063	c
CB(1)	0.1075 (13)	0.0898 (27)	0.2318 (13)	4.3	HB(3-2)	0.1711	−0.0173	0.2974	c
CB(2)	0.1403 (12)	0.1097 (28)	0.1753 (14)	5.5	HB(3-3)	0.1274	0.0674	0.3344	c
CB(3)	0.1494 (14)	0.0709 (28)	0.2944 (16)	6.7	HB(4-1)	0.0409	−0.0230	0.2592	c
CB(4)	0.0622 (15)	−0.0104 (35)	0.2220 (15)	8.1	HB(4-2)	0.0807	−0.1004	0.2141	c
N	−0.2459 (8)	0.5771 (18)	0.0861 (9)	2.7	HB(4-3)	0.0298	−0.0027	0.1794	c
P(1)	−0.2474 (3)	0.7086 (7)	0.1196 (4)	3.2	H(1-2)	−0.1684	0.5691	0.2148	c
P(2)	−0.2864 (3)	0.5007 (8)	0.0297 (4)	3.7	H(1-3)	−0.1633	0.5293	0.3298	c
C(1-1)	−0.2427 (11)	0.6910 (24)	0.2050 (11)	2.8	H(1-4)	−0.2272	0.6517	0.3876	c
C(1-2)	−0.1981 (12)	0.6122 (26)	0.2381 (14)	4.4	H(1-5)	−0.3026	0.7675	0.3393	c
C(1-3)	−0.1935 (13)	0.5910 (28)	0.3065 (15)	5.4	H(1-6)	−0.3006	0.8181	0.2189	c
C(1-4)	−0.2314 (14)	0.6571 (31)	0.3400 (15)	6.2	H(2-2)	−0.1611	0.6830	0.0359	c
C(1-5)	−0.2753 (13)	0.7336 (29)	0.3105 (15)	5.6	H(2-3)	−0.0776	0.7958	0.0168	c
C(1-6)	−0.2760 (11)	0.7528 (25)	0.2432 (13)	3.9	H(2-4)	−0.0496	0.9805	0.0769	c
C(2-1)	−0.1823 (11)	0.7984 (26)	0.1080 (12)	3.2	H(2-5)	−0.1039	1.0485	0.1584	c
C(2-2)	−0.1508 (13)	0.7599 (27)	0.0622 (13)	4.7	H(2-6)	−0.1874	0.9310	0.1803	c
C(2-3)	−0.0997 (15)	0.8304 (34)	0.0511 (16)	7.1	H(3-2)	−0.3730	0.7133	0.1306	c
C(2-4)	−0.0848 (14)	0.9332 (32)	0.0871 (16)	6.6	H(3-3)	−0.4532	0.8330	0.0833	c
C(2-5)	−0.1150 (15)	0.9704 (31)	0.1343 (16)	7.1	H(3-4)	−0.4439	0.9927	0.0114	c
C(2-6)	−0.1650 (12)	0.9039 (27)	0.1466 (12)	4.2	H(3-5)	−0.3534	1.0389	−0.0203	c
C(3-1)	−0.3116 (10)	0.8036 (22)	0.0850 (11)	2.1	H(3-6)	−0.2655	0.9245	0.0330	c
C(3-2)	−0.3678 (13)	0.7796 (26)	0.1004 (12)	4.2	H(4-2)	−0.3031	0.2983	−0.0704	c
C(3-3)	−0.4133 (12)	0.8488 (27)	0.0710 (13)	4.0	H(4-3)	−0.2403	0.1441	−0.1009	c
C(3-4)	−0.4080 (13)	0.9436 (29)	0.0304 (14)	5.2	H(4-4)	−0.1468	0.1121	−0.0305	c
C(3-5)	−0.3546 (15)	0.9710 (29)	0.0146 (14)	5.6	H(4-5)	−0.1106	0.2404	0.0512	c
C(3-6)	−0.3044 (12)	0.9002 (27)	0.0407 (12)	4.1	H(4-6)	−0.1669	0.4136	0.0783	c
C(4-1)	−0.2404 (11)	0.3834 (25)	0.0045 (12)	3.1	H(5-2)	−0.2306	0.6059	−0.0676	c
C(4-2)	−0.2627 (13)	0.2956 (31)	−0.0461 (15)	6.2	H(5-3)	−0.2640	0.7523	−0.1601	c
C(4-3)	−0.2252 (16)	0.1997 (34)	−0.0617 (16)	7.7	H(5-4)	−0.3600	0.8382	−0.1690	c
C(4-4)	−0.1710 (15)	0.1848 (32)	−0.0241 (17)	6.9	H(5-5)	−0.4331	0.7387	−0.1180	c
C(4-5)	−0.1518 (13)	0.2539 (31)	0.0254 (15)	5.6	H(5-6)	−0.3992	0.6180	−0.0215	c
C(4-6)	−0.1846 (12)	0.3565 (26)	0.0405 (12)	3.6	H(6-2)	−0.3195	0.4652	0.1556	c
C(5-1)	−0.3160 (10)	0.5965 (22)	−0.0402 (11)	1.9	H(6-3)	−0.3977	0.3688	0.1960	c
C(5-2)	−0.2710 (11)	0.6373 (27)	−0.0784 (13)	4.2	H(6-4)	−0.4640	0.2431	0.1220	c
C(5-3)	−0.2916 (12)	0.7251 (26)	−0.1302 (13)	4.1	H(6-5)	−0.4610	0.2319	0.0156	c
C(5-4)	−0.3476 (12)	0.7671 (25)	−0.1393 (12)	3.8	H(6-6)	−0.3936	0.3499	0.0353	c
C(5-5)	−0.3892 (13)	0.7193 (29)	−0.1045 (15)	5.6					

atom	β_{11}	β_{22}	β_{33}	β_{12}	β_{13}	β_{23}	atom	β_{11}	β_{22}	β_{33}	β_{12}	β_{13}	β_{23}
Fe(1)	174	799	230	8	9	−58	N(1)	197	643	273	−244	24	−226
Fe(2)	187	900	227	−94	11	−45	N(2)	257	1006	508	−236	198	181
Fe(3)	320	1057	265	105	101	−76	N(3)	437	1539	422	438	247	−139
Fe(4)	248	973	239	−176	83	2	N(4)	412	2277	421	−440	123	166
S(1)	293	1255	267	−88	48	−154	O(1)	415	1835	254	−132	46	−257
S(2)	230	1720	338	27	39	−50	O(2)	297	3391	586	−581	53	10
NA	260	746	242	−60	70	7	O(3)	680	1859	710	716	281	−69
NB	303	680	149	160	−8	20	O(4)	386	2233	427	−125	61	391

[a] Estimated standard deviations of the last significant figures are given in parentheses. [b] Anisotropic thermal parameters of the form $\exp[-(\beta_{11}h^2 + \beta_{22}k^2 + \beta_{33}l^2 + 2\beta_{12}hk + 2\beta_{13}hl + 2\beta_{23}kl)]$ were used. The resulting thermal coefficients ($\times 10^5$) are listed below. [c] Hydrogen atoms were assigned fixed isotropic thermal factors of 6.0 Å².

equivalent Fe_2SN faces are 2.565 (1) and 2.559 (1) Å. The mean of 2.562 Å is virtually identical with the calculated value of 2.57 Å obtained from an averaging of the Fe–Fe bond lengths for the Fe_2S_2 and $Fe_2(NR)_2$ fragments.

Under C_{2v} symmetry the two sets of equivalent Fe–S bond lengths have identical means of 2.22 Å, which is the same value as the mean of the 12 Fe–S bond lengths in $Fe_4(NO)_4(\mu_3\text{-}S)_4$. Likewise, the two sets of equivalent Fe–N bond lengths have identical means of 1.91 Å; this value compares favorably with Fe–N distances in other moleucles which contain triply bridging NR ligands—e.g., $Fe_3(CO)_9(\mu_3\text{-}NMe)_2$ (1.93 Å)[29] and $Fe_3(CO)_9(\mu_3\text{-}CO)(\mu_3\text{-}NSiMe_3)$ (1.90 Å).[31] Hence, no significant

Table IV. Distances and Bond Angles for $[(Ph_3P)_2N]^+[Fe_4(NO)_4(\mu_3\text{-}S)_2(\mu_2\text{-}NCMe_3)_2]^-$

A. Intraanion Distances (Å) with Those for the $Fe_4S_2N_2$ Core Averaged under Assumed C_{2v} Symmetry

Fe(1)-Fe(2)	2.552 (6)	Fe(3)-S(1)	2.256 (9)	S(1)···S(2)	3.494 (11)	N(1)-O(1)	1.211 (21)
Fe(3)-Fe(4)	2.701 (6)	Fe(4)-S(1)	2.244 (9)	NA···NB	2.788 (29)	N(2)-O(2)	1.214 (23)
		Fe(3)-S(2)	2.252 (9)			N(3)-O(3)	1.204 (27)
Fe(1)-Fe(3)	2.576 (6)	Fe(4)-S(2)	2.244 (10)	S(1)···NA	3.212 (21)	N(4)-O(4)	1.205 (28)
Fe(1)-Fe(4)	2.573 (6)		2.249 (av)	S(1)···NB	3.191 (21)		
Fe(2)-Fe(3)	2.570 (6)			S(2)···NA	3.193 (22)	NA-CA(1)	1.510 (30)
Fe(2)-Fe(4)	2.576 (6)	Fe(3)-NA	1.869 (20)	S(2)···NB	3.189 (22)	NB-CB(1)	1.595 (30)
	2.574 (av)	Fe(4)-NB	1.845 (20)		3.196 (av)		
			1.857 (av)			CA(1)-CA(2)	1.51 (4)
						CA(1)-CA(3)	1.53 (4)
Fe(1)-S(2)	2.254 (9)	Fe(1)-NA	1.889 (21)	Fe(1)-N(1)	1.622 (21)	CA(1)-CA(4)	1.50 (3)
Fe(2)-S(1)	2.265 (8)	Fe(2)-NA	1.898 (21)	Fe(2)-N(2)	1.595 (23)	CB(1)-CB(2)	1.50 (4)
	2.260 (av)	Fe(1)-NB	1.891 (19)	Fe(3)-N(3)	1.591 (28)	CB(1)-CB(3)	1.48 (3)
		Fe(2)-NB	1.888 (21)	Fe(4)-N(4)	1.625 (26)	CB(1)-CB(4)	1.48 (4)
			1.892 (av)				

B. Intraanion Bond Angles (deg) with Those for the $Fe_4S_2N_2$ Core Averaged under Assumed C_{2v} Symmetry

Fe(3)-S(1)-Fe(4)	73.8 (3)	S(1)-Fe(3)-S(2)	102.2 (4)	S(1)-Fe(2)-NA	100.6 (7)	NA-CA(1)-CA(2)	111 (2)
Fe(3)-S(2)-Fe(4)	73.8 (3)	S(1)-Fe(4)-S(2)	101.6 (4)	S(1)-Fe(2)-NB	100.0 (7)	NA-CA(1)-CA(3)	109 (3)
	73.8 (av)		101.9 (av)	S(2)-Fe(1)-NA	100.4 (7)	NA-CA(1)-CA(4)	108 (2)
				S(2)-Fe(1)-NB	100.2 (7)	NB-CB(1)-CB(2)	108 (2)
Fe(1)-S(2)-Fe(3)	69.9 (3)	NA-Fe(1)-NB	95.1 (9)		100.3 (av)	NB-CB(1)-CB(3)	107 (2)
Fe(1)-S(2)-Fe(4)	69.6 (3)	NA-Fe(2)-NB	94.9 (9)			NB-CB(1)-CB(4)	106 (2)
Fe(2)-S(1)-Fe(3)	69.5 (3)		95.0 (av)	Fe(1)-N(1)-O(1)	178 (2)		
Fe(2)-S(1)-Fe(4)	69.5 (3)			Fe(2)-N(2)-O(2)	174 (2)	CA(2)-CA(1)-CA(3)	112 (3)
	69.6 (av)	S(1)-Fe(3)-NA	102.3 (7)	Fe(3)-N(3)-O(3)	178 (3)	CA(2)-CA(1)-CA(4)	109 (3)
		S(1)-Fe(4)-NB	101.7 (7)	Fe(4)-N(4)-O(4)	176 (3)	CA(3)-CA(1)-CA(4)	108 (3)
Fe(1)-NA-Fe(2)	84.7 (9)	S(2)-Fe(3)-NA	101.4 (7)			CB(2)-CB(1)-CB(3)	111 (3)
Fe(1)-NB-Fe(2)	85.0 (9)	S(2)-Fe(4)-NB	101.7 (6)	Fe(1)-NA-CA(1)	128 (2)	CB(2)-CB(1)-CB(4)	115 (3)
	84.8 (av)		101.8 (av)	Fe(2)-NA-CA(1)	128 (2)	CB(3)-CB(1)-CB(4)	111 (3)
				Fe(3)-NA-CA(1)	128 (2)		
Fe(1)-NA-Fe(3)	86.5 (9)			Fe(1)-NB-CB(1)	127 (2)		
Fe(2)-NA-Fe(3)	86.1 (9)			Fe(2)-NB-CB(1)	126 (1)		
Fe(1)-NB-Fe(4)	87.0 (9)			Fe(4)-NB-CB(1)	130 (2)		
Fe(2)-NB-Fe(4)	87.3 (9)						
	86.7 (av)						

C. Intracation Distances (Å)

N-P(1)	1.57 (2)	C(1-5)-C(1-6)	1.40 (3)	C(3-1)-C(3-2)	1.40 (3)	C(5-1)-C(5-2)	1.46 (3)
N-P(2)	1.58 (2)	C(1-6)-C(1-1)	1.36 (3)	C(3-2)-C(3-3)	1.33 (3)	C(5-2)-C(5-3)	1.44 (3)
				C(3-3)-C(3-4)	1.33 (3)	C(5-3)-C(5-4)	1.34 (3)
P(1)-C(1-1)	1.75 (2)	C(2-1)-C(2-2)	1.35 (3)	C(3-4)-C(3-5)	1.35 (3)	C(5-4)-C(5-5)	1.38 (3)
P(1)-C(2-1)	1.82 (3)	C(2-2)-C(2-3)	1.44 (3)	C(3-5)-C(3-6)	1.40 (3)	C(5-5)-C(5-6)	1.36 (3)
P(1)-C(3-1)	1.82 (2)	C(2-3)-C(2-4)	1.34 (4)	C(3-6)-C(3-1)	1.41 (3)	C(5-6)-C(5-1)	1.34 (3)
P(2)-C(4-1)	1.77 (3)	C(2-4)-C(2-5)	1.34 (4)				
P(2)-C(5-1)	1.80 (2)	C(2-5)-C(2-6)	1.41 (3)	C(4-1)-C(4-2)	1.43 (3)	C(6-1)-C(6-2)	1.40 (3)
P(2)-C(6-1)	1.76 (2)	C(2-6)-C(2-1)	1.40 (3)	C(4-2)-C(4-3)	1.41 (4)	C(6-2)-C(6-3)	1.42 (3)
				C(4-3)-C(4-4)	1.35 (4)	C(6-3)-C(6-4)	1.35 (4)
C(1-1)-C(1-2)	1.40 (3)			C(4-4)-C(4-5)	1.28 (4)	C(6-4)-C(6-5)	1.28 (4)
C(1-2)-C(1-3)	1.41 (3)			C(4-5)-C(4-6)	1.39 (3)	C(6-5)-C(6-6)	1.41 (4)
C(1-3)-C(1-4)	1.39 (3)			C(4-6)-C(4-1)	1.39 (3)	C(6-6)-C(6-1)	1.43 (3)
C(1-4)-C(1-5)	1.35 (3)						

D. Intracation Angles (deg)

P(1)-N-P(2)	140 (1)	C(1-1)-P(1)-C(2-1)	106 (1)	P(1)-C(1-1)-C(1-2)	118 (2)	P(2)-C(4-1)-C(4-2)	122 (2)
		C(1-1)-P(1)-C(3-1)	111 (1)	P(1)-C(1-1)-C(1-6)	126 (2)	P(2)-C(4-1)-C(4-6)	122 (2)
N-P(1)-C(1-1)	110 (1)	C(2-1)-P(1)-C(3-1)	106 (1)	P(1)-C(2-1)-C(2-2)	118 (2)	P(2)-C(5-1)-C(5-2)	113 (2)
N-P(1)-C(2-1)	110 (1)	C(4-1)-P(2)-C(5-1)	109 (1)	P(1)-C(2-1)-C(2-6)	121 (2)	P(2)-C(5-1)-C(5-6)	124 (2)
N-P(1)-C(3-1)	114 (1)	C(4-1)-P(2)-C(6-1)	107 (1)	P(1)-C(3-1)-C(3-2)	121 (2)	P(2)-C(6-1)-C(6-2)	119 (2)
N-P(2)-C(4-1)	106 (1)	C(5-1)-P(2)-C(6-1)	108 (1)	P(1)-C(3-1)-C(3-6)	119 (2)	P(2)-C(6-1)-C(6-6)	124 (2)
N-P(2)-C(5-1)	113 (1)						
N-P(2)-C(6-1)	113 (1)						

differences are observed in either the Fe–S or Fe–N distances contained in the Fe_2S_2 or Fe_2N_2 faces relative to those in the Fe_2SN faces, and furthermore, these bond lengths are analogous with those for the corresponding ligands coordinated to *three* iron atoms (vs. significantly longer distances for the same ligands attached to only two iron atoms).

The three independent nitrosyl ligands are coordinated to the iron atoms in a normal pattern. The Fe–NO bond lengths vary from 1.653 (6) to 1.668 (6) Å; the mean value of 1.66 Å is similar to that found in $Fe_4(NO)_4(\mu_3\text{-}S)_4$ (1.66 Å),[1] $Fe_2(NO)_4(\mu_2\text{-}SEt)_2$ (1.67 Å),[32] and $Fe_2(NO)_4(\mu_2\text{-}I)_2$ (1.67 Å)[33] and in the $[Fe_4(NO)_7(\mu_3\text{-}S)_3]^-$ monoanion.[10] The degree of linearity of the Fe–N–O bond angles in $Fe_4(NO)_4(\mu_3\text{-}S)_2(\mu_3\text{-}NCMe_3)_2$ (range (177.8 (4)–179.4 (7)°) parallels that found in $Fe_4(NO)_4(\mu_3\text{-}S)_4$ (range 176.9 (5)–178.7 (5)°) as well as that of 176.3 (9)° determined[10] for the apical $S_3Fe(NO)$ fragment in the $[Fe_4(NO)_7(\mu_3\text{-}S)_3]^-$ monoanion, in sharp contrast to the much greater deviations of the Fe–N–O bond angles from linearity found for the $Fe(NO)_2$ fragments in $Fe_2(NO)_4(\mu_2\text{-}SEt)_2$ (identical values of 167 (3)°),[32] in $Fe_2(NO)_4(\mu_2\text{-}I)_2$ (range 157 (3)–165 (3)°),[33] and in the $[Fe_4(NO)_7(\mu_3\text{-}S)_3]^-$ monoanion (range 164.6 (9)–171.0

(31) Barnett, B. L.; Krüger, C. *Angew. Chem., Int. Ed. Engl.* **1971**, *10*, 910–911.

(32) Thomas, J. T.; Robertson, J. H.; Cox, E. G. *Acta Crystallogr.* **1958**, *11*, 599–604.

(33) Dahl, L. F.; Rodulfo de Gil, E.; Feltham, R. D. *J. Am. Chem. Soc.* **1969**, *91*, 1653–1664.

Table V. Selected Mean Distances and Bond Angles for $[Fe_4(NO)_4(\mu_3\text{-}S)_2(\mu_3\text{-}NR)_2]^n$ ($n = 0, -1$; $R = C(CH_3)_3$) Containing an $[Fe_4S_2N_2]^n$ Core Approximately Conforming to C_{2v}–$2mm$ Symmetry[a,b]

core dimension	core fragment[c]	[]d	1, $[Fe_4S_2N_2]^0$	2, $[Fe_4S_2N_2]^-$	difference,[e] $\Delta = \bar{x}_2 - \bar{x}_1$	$\lvert\Delta\rvert/\sigma$[f]
			Distance, Å			
Fe-Fe	Fe_2S_2	[1]	2.642 (1)	2.701 (6)	+0.059*	9.7
	Fe_2SN	[4]	2.562 (3)	2.574 (1.4)	+0.012	3.6
	Fe_2N_2	[1]	2.496 (1)	2.552 (6)	+0.056*	9.2
S···S	Fe_2S_2	[1]	3.507 (3)	3.494 (11)	−0.013	1.1
S···N	Fe_2SN	[4]	3.208 (0.5)	3.196 (5.3)	−0.01	1.9
N···N	Fe_2N_2	[1]	2.880 (7)	2.788 (29)	−0.09	3.0
Fe-S	Fe_2S_2	[4]	2.224 (3.5)	2.249 (3)	+0.025*	5.4
	Fe_2SN	[2]	2.222 (2)	2.260 (5.5)	+0.038*	6.5
Fe-N	Fe_2SN	[2]	1.914 (3)	1.857 (12)	−0.06*	4.8
	Fe_2N_2	[4]	1.908 (3.5)	1.892 (4.5)	−0.02	3.5
			Angles, deg			
Fe-S-Fe	Fe_2S_2	[2]	72.9 (1.2)	73.8 (0)	+0.9*	7.2
	Fe_2SN	[4]	70.4 (0.6)	69.6 (1)	−0.8*	7.3
Fe-N-Fe	Fe_2SN	[4]	84.2 (2.5)	86.7 (3)	+2.5*	6.8
	Fe_2N_2	[2]	81.6 (1)	84.8 (2)	+3.2*	17.8
S-Fe-S	Fe_2S_2	[2]	104.0 (1)	101.9 (3)	−2.1*	6.6
S-Fe-N	Fe_2SN	[4]	101.6 (1)	100.3 (1.3)	−1.3*	8.0
	Fe_2SN	[4]	101.4 (1)	101.8 (1.9)	+0.4	1.9
N-Fe-N	Fe_2N_2	[2]	98.0 (2)	95.0 (0.1)	−3.0*	14.8

[a] The $[Fe_4S_2N_2]^0$ and $[Fe_4S_2N_2]^-$ cores have crystallographic site symmetry C_s–m and C_1–1, respectively. [b] Each esd given in parentheses represents the standard deviation of the mean, $\sigma(\bar{x}) = s/n^{1/2}$, where $s = [\Sigma(x_n - \bar{x})^2/(n-1)]^{1/2}$ corresponding to the root-mean-squared esd of an individual sample point of n measurements. [c] Designates that part of the $Fe_4S_2N_2$ core pertaining to a given distance or bond angle. [d] Brackets enclose the number of equivalent distances or bond angles having the values listed in the right columns. [e] The asterisks denote dimensional differences, $\bar{x}_2 - \bar{x}_1$, which are considered to be significantly meaningful on an arbitrary basis that $\lvert\Delta\rvert/\sigma \geq 5$. [f] $\lvert\Delta\rvert/\sigma = \lvert\bar{x}_2 - \bar{x}_1\rvert/[\sigma(\bar{x}_1)^2 + \sigma(\bar{x}_2)^2]^{1/2}$, where $\sigma(\bar{x}_1)$ and $\sigma(\bar{x}_2)$ are the standard deviations of the means.

(9)°).[10] Since a nitrosyl bending distortion (superimposed on that due to packing effects) is expected from qualitative electronic considerations[34] when the local symmetry about an Fe–NO fragment is less than C_3, it is concluded that the bridging S and NR ligands in $Fe_4(NO)_4(\mu_3\text{-}S)_2(\mu_3\text{-}NCMe_3)_2$ are not sufficiently different in their electronic interactions with a given iron atom such that a pseudo-C_3 local symmetry at each iron atom is preserved. This results in the energy difference between the two normally degenerate π^*(NO) orbitals (under regular C_3 site symmetry) of a nitrosyl ligand being sufficiently small (and likewise that between the two corresponding π(NO) orbitals) that their nearly equivalent electron populations prevent a significant geometrical distortion of the nitrosyl ligand from linearity.

In this connection, an extensive Mössbauer spectroscopic investigation of both $Fe_4(NO)_4(\mu_3\text{-}S)_2(\mu_3\text{-}NCMe_3)_2$ and $Fe_4(NO)_4(\mu_3\text{-}S)_4$ was carried out by Sedney and Reiff[35] in an effort to distinguish between the two types of local iron environments in the former compound by the expectation of four-line Mössbauer spectra. However, least-squares analysis[35] of the high-resolution, zero-field data from 1.6 to 300 K for the $Fe_4S_2(NR)_2$ nitrosyl cluster and from 4.2 to 300 K for the Fe_4S_4 nitrosyl cluster resulted in markedly similar spectra consisting in each case of a single, symmetrical quadrupole doublet throughout the temperature range. It was concluded[35] that the four iron sites in each cluster possess equivalent environments on a Mössbauer time scale. Applied high-field spectra from 0 to 60 kG of both compounds were also found to be essentially identical, thereby providing further evidence that "the *tert*-butyl nitrogen and sulfur ligands are apparently sufficiently similar to produce comparable ligand fields at the iron nucleus".[35] It is also noteworthy that, although the high-field spectra of both compounds lead to an internal hyperfine field of zero, as expected for a diamagnetic ground state, magnetic susceptibility measurements[35] indicate that both clusters exhibit a small degree of paramagnetic character. This is evidenced by a decrease in the magnetic moment per iron from 0.76 to 0.52 μ_B for the Fe_4S_4 cluster and from 0.89 to 0.62 μ_B for the $Fe_4S_2(NR)_2$ cluster over a temperature range of 300 to 50 K for both compounds.

Stereochemical Comparison between the $[Fe_4(NO)_4(\mu_3\text{-}S)_2(\mu_3\text{-}NCMe_3)_2]^-$ Monoanion and $Fe_4(NO)_4(\mu_3\text{-}S)_2(\mu_3\text{-}NCMe_3)_2$. Of prime interest from a bonding viewpoint is an analysis of the changes in geometry of the neutral parent upon reduction to the monoanion. The monoanion (Figure 5) retains the idealized C_{2v}—$2mm$ geometry with no imposed crystallographic constraints.

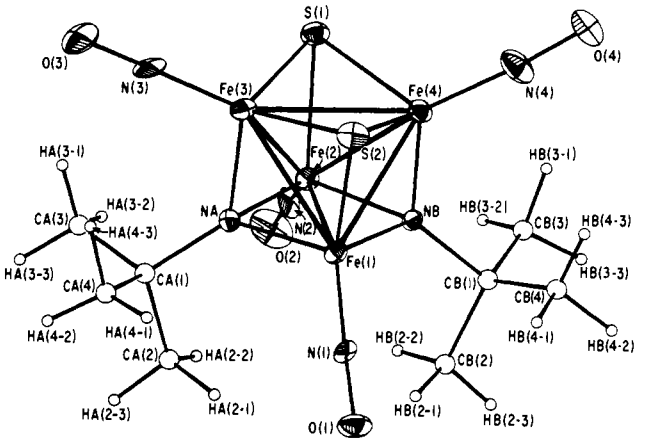

Figure 5. View of the $[Fe_4(NO)_4(\mu_3\text{-}S)_2(\mu_3\text{-}NCMe_3)_2]^-$ monoanion which has an idealized C_{2v} geometry with no crystallographically required symmetry.

On going from the neutral molecule to the monoanion, the major observed structural changes of significance (Table V) are the relatively large increases in distance of 0.059 Å between the iron atoms in the Fe_2S_2 fragment and of 0.056 Å between the iron atoms in the Fe_2N_2 fragment in contrast to the small average increase in distance of 0.012 Å between the iron atoms in each of the four equivalent Fe_2SN fragments. This preferential lengthening of the two Fe–Fe bonds normal to the C_2—2 axis in the monoanion is presumed to be the major driving force which gives rise to significant differences in other distances and bond angles between the two C_{2v} $Fe_4S_2N_2$ frameworks (Table V). The four equivalent Fe–S bonds in the Fe_2S_2 fragment and the two equivalent Fe–S bonds in the Fe_2SN fragments are both found to be *longer* in the monoanion by 0.025 and 0.038 Å, respectively, whereas the corresponding four equivalent Fe–N bonds in the Fe_2N_2 fragment and the two equivalent Fe–N bonds in the Fe_2SN fragments are both found to be *shorter* in the monoanion by 0.016 and 0.057 Å, respectively. There is no apparent rationalization

(34) Enemark, J. H. *Inorg. Chem.* **1971**, *10*, 1952–1957.
(35) Sedney, D.; Reiff, W. M. *Inorg. Chim. Acta* **1979**, *34*, 231–236.

from electronic considerations either for the occurrence of these opposite variations in the Fe–S and Fe–N bond lengths between the neutral molecule and monoanion or for these opposite changes not being primarily restricted to the Fe_2S_2 and Fe_2N_2 fragments.

The lengthening of the Fe–Fe distances in the monoanion also gives rise to small but significant changes in the two kinds of Fe–S–Fe bond angles of +0.9° and −0.8° and in the two kinds of Fe–N–Fe bond angles of +2.5° and +3.2°. The Fe–NO, N–O, and N–C bond distances are not significantly different in terms of their esd's.

Bonding Description of the $[(Fe_4(NO)_4(\mu_3\text{-}S)_2(\mu_3\text{-}NCMe_3)_2]^n$ Series (n = 0, −1). A molecular orbital approach is necessary in order to rationalize the observed differences in the Fe–Fe distances of the monoanion and neutral species. A qualitative MO metal cluster model[3] applied[1] to $Fe_4(NO)_4(\mu_3\text{-}S)_4$ produces under cubic T_d—$\bar{4}3m$ symmetry the electronic configuration $(e + t_1 + t_2)^{16}(a_1 + e + t_2)^{12}(t_1 + t_2)^0$ involving 28 valence electrons from the four d^7 Fe(I) atoms completely occupying six strongly bonding $(a_1 + e + t_2)$ tetrairon levels with no electrons in the corresponding antibonding $(t_1 + t_2)$ tetrairon levels. The filled lower energy $(e + t_1 + t_2)$ tetrairon symmetry orbitals are not involved in direct Fe–Fe interactions but are stabilized primarily by the π^*(NO) orbitals of the π-acidic nitrosyl ligands. Upon the addition of one electron to $Fe_4(NO)_4(\mu_3\text{-}S)_4$ to form the reduced monoanion, one of the two triply degenerate antibonding levels (viz., t_1 or t_2) will be only partially occupied, and hence a first-order Jahn–Teller distortion is presumed to occur in which the idealized cubic T_d molecular geometry may undergo a vibronically allowed tetragonal distortion to give a D_{2d}—$\bar{4}2m$ geometry. Since the neutral molecule has 12 electrons in the six bonding metal cluster orbitals (corresponding to a total bond order of 6.0 or a bond order of 1.0 per Fe–Fe bond), the addition of one antibonding electron produces a decrease of 0.5 in the *total* metal–metal bond order. A splitting of the partially occupied triply degenerate level under tetragonal D_{2d} symmetry into a lower energy nondegenerate level containing the unpaired electron and an empty, higher energy doubly degenerate level may result in two different limiting configurations for the monoanion. For the first limiting electronic configuration, the two equivalent Fe–Fe bonds normal to the S_4 axis retain individual bond orders of 1.0 while each of the other four equivalent Fe–Fe bonds will *lengthen* in order to decrease its bond order from unity to a value of $^7/_8$ (corresponding to a *total* bond order decrease of $^4/_8$ or 0.5). For the second limiting configuration the four latter Fe–Fe bonds retain individual bond orders of unity while the two Fe–Fe bonds normal to the S_4 axis will *lengthen* in order to decrease their individual bond orders from unity to $^3/_4$ (corresponding again to a 0.5 *total* bond-order change).

This delocalized metal cluster description can be conceptually carried over to the electronically equivalent $Fe_4(NO)_4(\mu_3\text{-}S)_2(\mu_3\text{-}NCMe_3)_2$ molecule even though the dissimilarity between the triply bridging sulfur and *N-tert*-butyl ligands lowers the molecular symmetry to C_{2v}. The important structural feature in the neutral $Fe_4(NO)_4(\mu_3\text{-}S)_2(\mu_3\text{-}NCMe_3)_2$ is that the Fe–Fe bond lengths are in accord with a completely bonding iron tetrahedron, which implies that there are six electron pairs occupying the six bonding tetrairon symmetry orbitals, with the corresponding higher energy antibonding ones being empty. In the $[Fe_4(NO)_4(\mu_3\text{-}S)_2(\mu_3\text{-}NCMe_3)_2]^-$ monoanion, the MO metal cluster model predicts that the additional electron occupies an antibonding tetrairon symmetry orbital, thereby analogously resulting in a decrease of the *total* metal–metal bond order from 6.0 to 5.5. The observed preferential lengthening under C_{2v} symmetry of only two of the six Fe–Fe distances indicates that the bond-order distribution in the monoanion can be considered under a localized tetrairon approximation to correlate with the Fe–Fe bonds in the Fe_2S_2 and Fe_2N_2 fragments each possessing a bond order of $^3/_4$ while the Fe–Fe bonds in the four Fe_2SN fragments each retain a bond order of 1.0.

Although this localized bond-order description is not incompatible with the observed Fe–Fe distances in the monoanion relative to those in the neutral parent, it is important to note that the MO model in general involves the distribution of electrons in delocalized metal symmetry orbitals such that only the total metal–metal bond order is obtained from the model. The partitioning of the total metal–metal bond order for the metal cluster into individual localized bond orders on the basis of the determined metal–metal distances is an arbitrary assignment and is not necessarily clear-cut in all complexes (i.e., the antibonding metal cluster electrons may not be purely antibonding between only certain pairs of metal atoms).

Since the $[Fe_4(NO)_4(\mu_3\text{-}S)_2(\mu_3\text{-}NCMe_3)_2]^-$ monoanionc is the only structurally known example to date of the so-called 13-electron tetrahedral-like metal system with 12 bonding and one antibonding metal cluster electrons, further research, including structural investigations, is needed to provide more observables for testing and extending this metal cluster model.

Acknowledgment. We are most grateful for the financial support of this research by the National Science Foundation.

Registry No. $Fe_4(NO)_4(\mu_3\text{-}S)_2(\mu_3\text{-}NCMe_3)_2$, 53276-79-2; $[(Ph_3P)_2N]^+[Fe_4(NO)_4(\mu_3\text{-}S)_2(\mu_3\text{-}NCMe_3)_2]^-$, 80399-52-6; $Hg[Fe(CO)_3NO]_2$, 28411-05-4; $(Me_3CN)_2S$, 2056-74-8.